

# Hyperspectral Remote Sensing in Characterizing Soil Salinity Severity using SVM Technique - A Case Study of Alluvial Plains

Justin George K. and Suresh Kumar

Agriculture and Soils Department, Indian Institute of Remote Sensing, ISRO, Dehradun, Uttarakhand, India

Publication Date: 23 October 2015

Article Link: <http://technical.cloud-journals.com/index.php/IJARSG/article/view/Tech-461>



Copyright © 2015 Justin George K. and Suresh Kumar. This is an open access article distributed under the **Creative Commons Attribution License**, which permits unrestricted use, distribution, and reproduction in any medium, provided the original work is properly cited.

**Abstract** Hyperspectral remote sensing is widely used for analyzing and estimating the severity of soil salinity in arid and semi-arid regions, throughout the world. The present study is an attempt to map the various soil salinity severity classes using different hyperspectral indices generated using EO-1 Hyperion data and Support Vector Machine (SVM) method, in the Mathura region of Indo-Gangetic plain of India. Various hyperspectral indices such as Soil Adjusted Vegetation Index (SAVI), Desertification Soil Index (DSI), Salinity Index (SI) and Normalized Difference Water Index (NDWI) were chosen, generated and effectively used for characterizing and mapping soil salinity severity. Salt infestation in the study area was categorized into four classes of normal, slight, moderate, high soil salinity. Hyperspectral indices helped in identification of various features like vegetation, waterlogged area and soil areas under various classes of soil salinity. The salinity index and desertification soil indices were found to respond well to varying degrees of soil salinity. The SVM technique generated soil salinity map with overall classification accuracy of 78.13 percent, with a kappa statistic of 0.71. The results indicated highest accuracy in high soil salinity class in comparison to other classes, attaining producers and users accuracies of 85.71% and 90.0% respectively. Slight saline class showed poor producers and users accuracy. The result showed high accuracy for mapping soil salinity severity with machine learning classifier like SVM using various indices generated from hyperspectral remote sensing data. These generated images can be effectively used in planning of various management practices and effective reclamation measures of salt affected soils.

**Keywords** *Hyperion Hyperspectral Indices; Indo-Gangetic Plains; Salt Salinity Severity; Support Vector Machine (SVM)*

## 1. Introduction

Unplanned and unscientific exploitation of land resources to fulfill ever increasing human needs have resulted in huge pressure on limited soil resources leading to land degradation. Salinization, alkalization, waterlogging and loss of soil organic matter are the major processes which causes degradation and leading to formation of degraded lands. Soil salinity is one of the main environmental factors that adversely affect plant growth and development. Salinization and alkalization processes resulting in salt-affected soils (Metternicht and Zinck, 2003) are major cause of land degradation in the

hot arid and semi-arid regions where majority of agricultural lands comes under irrigation. These arid and semi-arid regions experience very low amount of precipitation which makes impossible for maintaining a regular percolation of water through the soil and the subsequent removal of excessive soluble salts. Under such a climatic condition, soluble salts get accumulated in the surface soil, thus negatively influencing soil properties and environment ultimately resulting in lowering of soil productivity. The consistent identification of salinity forming processes and areal extent of salinity are very much essential for sustainable soil management. Salt affected landscapes are very sensitive to changes in climatic, edaphic and hydrological conditions in time and space.

Salinization affects about 30% of the world's total irrigated land and decreases this area approximately 1-2% per year due to salt infestation (FAO, 2002). Indo-Gangetic plains, major food producing zone of the country occupies nearly 49.3 Mha, of which 2.5 Mha land are under various degrees of degradation because of salinization and alkalization occurring in the hot arid and semi-arid climates (Abrol and Bhumbla, 1971). This salt affected area comes to nearly 25% of the total salt affected area (10.1 Mha) of the country. These lands have high concentrations of neutral and alkaline soluble salts in the surface and sub-surface soil layers due to additions from the continuous irrigation with water containing dissolved salts or salts present at lower depth of the soil transported to the surface (Szabolcs, 1989), mainly due to capillary rise and subsequent evaporation from the soil surface. These salts adversely influence the various soil properties and thus results in reduction of crop growth, crop yields, land productivity and leads to land degradation ultimately (Oosterbaan, et al., 1990; Dehaan and Taylor, 2002; Shahbaz and Ashraf, 2013). Information regarding the spatial distribution, severity and temporal expansion of salinity are critical for monitoring, planning and implementation of various management strategies for the reclamation of these soils.

Traditional methods for identifying and monitoring of salt affected soils can map soil salinity severity only up to a certain extent. They are expensive, time consuming and require large number of samples from an area to characterize spatial variability, which restrict the adoption of these methods for studying large and non-uniform areas (Shepherd and Walsh, 2002). Various remote sensing data are being widely used in characterization and mapping of salt affected soils including aerial photographs, multispectral and hyperspectral remote sensing data (Mitran, et al., 2015). Soil salinity mapping is a difficult task to perform because of the high influence of various soil physical and chemical properties (e.g. moisture, surface roughness, organic matter) on soil reflectance (Ben-Dor, et al., 2002; Shrestha, et al., 2005). Earlier, monitoring and mapping of salt affected lands in relatively large areas were widely and successfully undertaken using broadband multispectral data (Toth, et al., 1991; Mougnot and Pouget, 1993). But nowadays, use of broadband multispectral data for soil salinity studies is very less and restricted because of spatial and spectral resolution limitations that mask details in the spectral signatures of various kinds of salt-affected lands (Allbed and Kumar, 2013). Various problems are also there which interfere in the detection of salt-affected soils using remote sensing, i.e. sometimes the process goes undetected, especially when the soils are not fully affected by salt minerals, the physical boundaries separating areas of different degrees of salinity are fuzzy, the salinization process occurs throughout the soil profile along with soil surface, which the optical sensors cannot detect (Ghosh, et al., 2012). These limitations calls for the use of hyperspectral remote sensing data in soil salinity studies for better detection and mapping, because of its ability to identify characteristic absorption bands in salt affected soils and the associated minerals and related spectral features (Csillag, et al., 1993; Farifteh and Van der Meer, 2005; Shi and Huang, 2007)

The mapping of salt-affected soils using hyperspectral satellite data has been investigated by several workers like Taylor and Dehaan (2003) and Dutkiewicz, et al. (2009). Dehaan and Taylor (2002) evaluated the utility of field-derived spectra of saline soils and related vegetation for characterizing and mapping the spatial distribution of irrigation-induced soil salinization. Wu, et al. (2010) used Artificial Neural Network (ANN) and Support Vector Machine (SVM) classification methods for mapping land degradation using Hyperion data and found that SVM classification achieved higher accuracy than

ANN method. Ghosh, et al. (2012) has successfully used linear unmixing and SAM methods for mapping soil salinity using Hyperion remote sensing data. This spectral unmixing technique helps in mapping of fractions of various salt classes in each pixel. Hamzeh, et al. (2012) investigated the ability of hyperspectral Hyperion data for mapping salinity stress in sugarcane fields. They used different classifications such as Support Vector Machine (SVM), Spectral Angle Mapper (SAM), Minimum Distance (MD) and Maximum Likelihood (ML) with different band combinations and classified soil salinity into three classes (low, moderate and high salinity). Their results indicated that salinity map generated by SVM classification, using all bands as input data yielded good accuracy compared to other methods. SVMs are highly appealing in the field of remote sensing because of their ability to handle small training data sets successfully, often producing higher classification accuracy compared to the methods used traditionally (Mantero, et al., 2005) The benefit of SVMs is because of the learning process, which follows what is known as structural risk minimization. Under this, classification error on unseen data is minimized by SVMs without any prior assumptions made on the probability distribution of the data. Taking all these factors into consideration, the present study was undertaken with the objective of (i) mapping soil salinity severity in the area using SVM technique. Various spectral indices generated using hyperion hyperspectral remote sensing data served as input data layers for carrying out mapping using SVM technique.

## 2. Study Area

The study area is a part of Indo-Gangetic plains and lies between  $26^{\circ}76'$  N to  $27^{\circ}62'$  N latitudes and  $77^{\circ}31'E$  to  $77^{\circ}59'E$  longitudes in Mathura district of Uttar Pradesh, India (Figure 1). The area experiences semi-arid climate with intense hot summers, cold winter and general dryness throughout the year except during south-west monsoon period from July to September. The mean annual temperature is  $24.4^{\circ}\text{C}$ ; maximum temperature in May goes up to  $45^{\circ}\text{C}$  and mean minimum temperature up to  $14^{\circ}\text{C}$  in the month of January. The average annual rainfall is 505 mm and 92 % of it is received during the rainy season comprising July, August and September months of the year. The area is an irrigation command area and has a good network of irrigation canals, distributaries and minors to irrigate the fields. The Yamuna River passes very close to the area. The soils in the area are developed over the alluvium deposited by Yamuna River. The landscape is nearly level to very gentle sloping with moderate to poor surface drainage. The surface soil texture in the area ranged from silt loam to clay loam. The salt affected soils in the area are characterized as saline-alkali soils and belong to Fine Loamy Typic Natrustalfs and Typic Ustepts families. These lands are intensively cultivated for wheat, rice, mustard, sugarcane, sorghum, etc. crops with irrigation facilities from canals and wells, irrespective of their high salinity status.

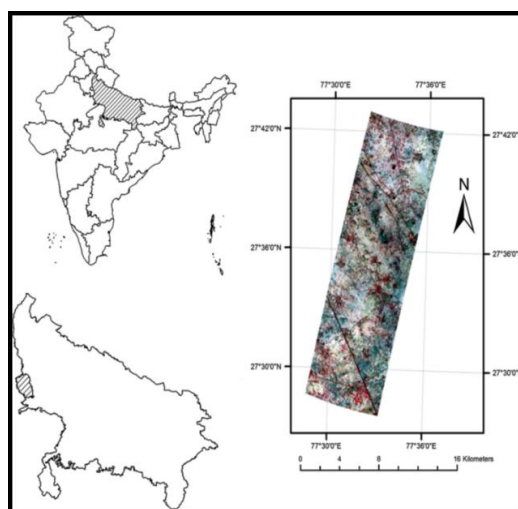


**Figure 1:** Location Map of the Study Area

### 3. Material and Methods

#### 3.1. Satellite Data Used

- 1) Space borne hyperspectral remote sensing data (EO-1 Hyperion) acquired on May 5, 2005 was used for the study (Table 1), as it's the summer month and fields are clear with no crop. The Level 1 radiometric (L1R) product used in the study had 242 bands with a spectral resolution of 10 nm, spatial resolution of 30 m and 12 bit radiometric quantization. Only 196 bands out of 242 bands were calibrated. These bands belong to visible-to-near-infrared (VNIR) (bands 8–57) and shortwave-infrared (SWIR) wavelength regions (bands 77–24) (Datt, et al., 2003). All bands were not calibrated due to low detector response and uncalibrated bands thus were set to zero.

**Table 1: Hyperion Sensor (EO-1) Characteristics**

EO-1 launched	21 November 2000
Altitude	705 km
Swath	7.5 km
Spatial resolution	30 meter
Spectral band width	10 nm (nominal)
Radiometric resolution	12 bits
Spectral channels	220 unique channels
VNIR range	70 channels, 356-1058 nm
SWIR range	172 channels, 852-2577 nm
No. of columns	3400
No. of lines	256
Instantaneous field of view (IFOV)	42.4 microradian

- 2) Indian Remote Sensing (IRS) LISS IV (Linear Imaging Self Scanner) satellite data: The data acquired on May 6, 2007 (Table 2) and standard false color composite (FCC) at 1:25,000 scale was generated for visual interpretation of salt affected soils and to locate these soils for soil sampling during field survey.

**Table 2: IRS P6 Sensor Specifications**

Altitude (km)	817
Spatial resolution (m)	5.8
Swath (km)	23.9 (Mx)
Spectral bands	B2: 0.52-0.59 B3: 0.62-0.68 B4: 0.77-0.86
Quantization (bits)	7
Sensor	Push broom
Focal length (mm)	982
Repeat cycle (days)	5

#### 3.2. Software Used

ENVI 5.0 (Environment for Visualizing Images, Research System, Inc) software was used for digital image analysis of the hyperspectral satellite data. It offers "Hyperion tool kit" to analyze hyperspectral satellite data. ERDAS Imagine 9.2 ver. Image processing software was used for the accuracy assessment of spectral index classified images. ArcGIS 10.0 developed by ESRI, Inc. was also used for visualization of final maps.

#### 4. Methodology

The brief methodology adopted for the present study is shown in Figure 2.

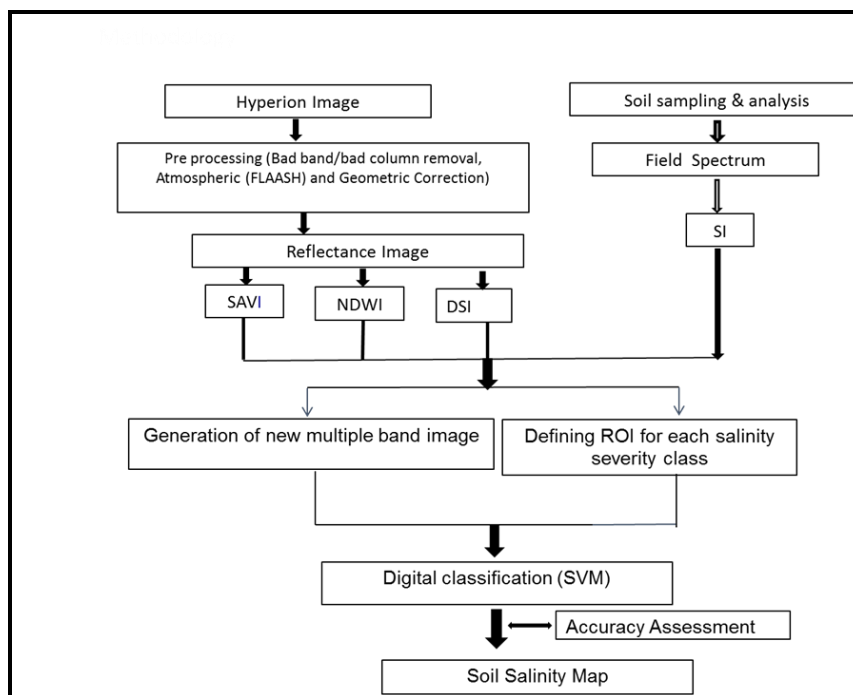


*Figure 2: Brief Methodology Adopted in the Study*

#### 4.1. Hyperion Data Processing

Hyperion data is initially processed by the EO-1 product generation system (EPGS) and distributed in different processing levels. In this study, radiometrically corrected level 1R product (L1R) of Hyperion has been used.

The “Hyperion tool kit” was used to import the L1R product from HDF format to ENVI standard format in ENVI 5.0 (Environment for Visualizing Images, Research System, Inc). The flag Mask correction option available in the tool kit was used to correct vertical stripping, stripping was removed by replacing the bad values with the average of the good values on either side of them (Figure 3). The image was then visually checked to identify the left over bad columns. Out of the calibrated bands of Hyperion (band 8 to band 55, band 56 and band 57, band 79 to band 224), 152 bands from 196 unique bands were selected by spectral subsetting. Bands in the high water absorption range from 1400 nm to 1900 nm and bands which had high acceptable noise and streaking were removed from further processing. These selected bands were again visually inspected for bad columns to eliminate the stripping errors (Table 3).

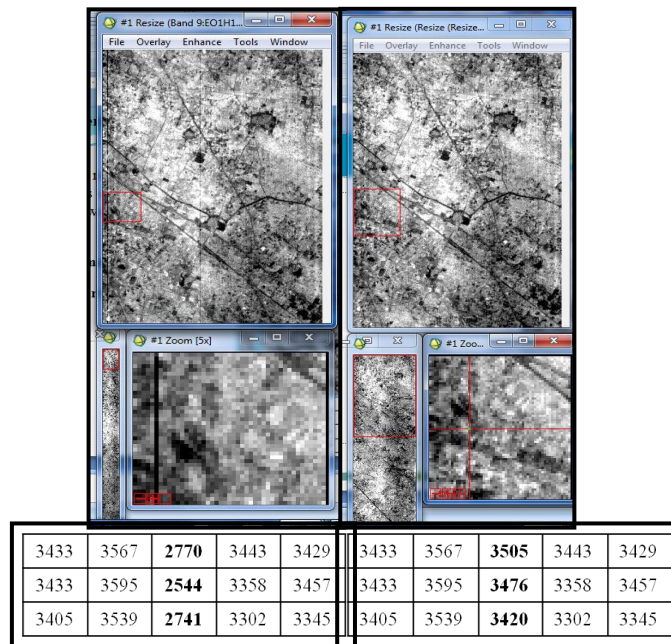


**Figure 3:** Hyperion Level 1R Band 9 of Mathura Dataset (A) Band With Stripes With Low DN Values in Bold (B) De-Striped Band With Changed DN Values after Applying Local Filter

**Table 3:** Location of Bad Columns in Spectrally Subsetted L1R Product

Bands	Bad Columns
9	6,10,12,13,67,68, 114
10	114, 199
27	46,47
20	19,20
54	22,23,24,25
55	12,13,24,25
56	10,11,12,13,17,19,24,36,37,38,39
83	59,94,95,120,121
84	48,49,58,70,71,86,87,88,94,95,234
87	233,234
88	25,51,52,76,99,100,144,145,157,204,
97	35,36,79,80,88,89,116,117,118,157,158
99	15,16,34,35,49,50,51,61,62,73,74,129,130,131,155,156,246,249,250
100	26,38,51,52,67,68,87,88,203,204,228,229,247,248
102	8,27,32
118	16,222,223
133	16,36,174,253,254,255
195	50,56,57
83-119	256
133-164	256
183-184	256
188-220	256

#### 4.2. Atmospheric Correction

Remote sensing measurements of the Earth’s surface are strongly influenced by atmosphere. Water vapour with smaller contributions from carbon dioxide, ozone and other gases dominates the absorption by atmospheric gases. In order to only retrieve the surface reflectance and study the reflectance properties, the atmospheric components have to be removed. In the study area, ENVI’s

Fast Line-of-sight Atmospheric Analysis of Spectral Hyper-cubes (FLAASH) module was applied on Hyperion data for atmospheric correction. The various parameters used in FLAASH atmospheric correction are given in Table 4. FLAASH is a first-principles atmospheric correction tool that corrects wavelengths on the visible through near-infrared and shortwave infrared regions up to 3  $\mu\text{m}$ . FLAASH requires input image in BIL format and ASCII file of scale factors number. The scale factors for the VNIR and SWIR bands are 400 and 800 respectively in the case of nanometers (nm) while 40 and 80 for  $\mu\text{m}$ . The study area is rural and it falls in tropical climate. Thus, tropical atmospheric and rural aerosol model of FLAASH were selected and other parameters were defined based on metadata of the Hyperion image File. The change in the spectral reflectance curve of vegetation area before and after FLAASH correction can be seen in Figure 4.

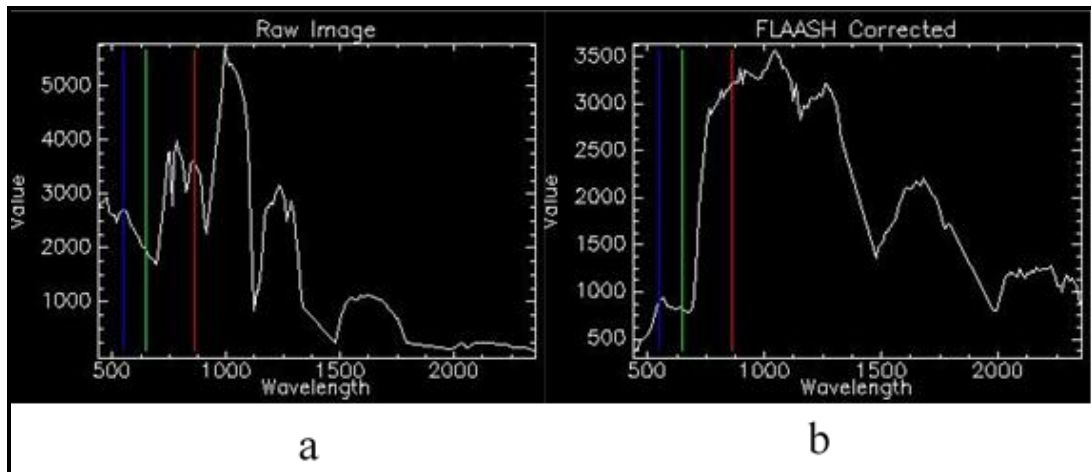


Figure 4: Spectral Curve of Vegetation (a) before FLAASH and (b) after FLAASH

Table 4: Parameters used in FLAASH Atmospheric Correction

Parameter		Parameter	
Scene Center Location	27.2, 77.45	Initial visibility	40 km
Sensor Altitude	705km	Spectral polishing	Yes
Ground Elevation	0.18m	Width(no. of bands)	9
Pixel Size	30m	Wavelength Recalibration	No
Flight Date	15.5.2005	Aerosol Retrieval Height	1.5km
Flight Time	5h 11m 58sec	CO <sub>2</sub> Mixing Ratio (ppm)	390ppm
Atmospheric Model	Tropical	Use Adjacency correction	Yes
Water Retrieval	Yes	Modtran resolution	5 cm <sup>-1</sup>
Water Absorption Feature	1135nm	Modtran Multiscatter Model	Scaled-DISORT
Aerosol Model	Rural	No. of Disort streams	8
Aerosol Retrieval	None	Output reflectance factor	10000

### 4.3. Geometric Correction

The satellite images (Hyperion and LISS-IV) were geometrically registered with geo-referenced Landsat ETM+ / SOI toposheet (1:50,000) using nearest neighbor resampling with first order polynomial equation. The image was projected with Lambert Conformal Conic projection in WGS-84 spheroid and datum (Figure 5).

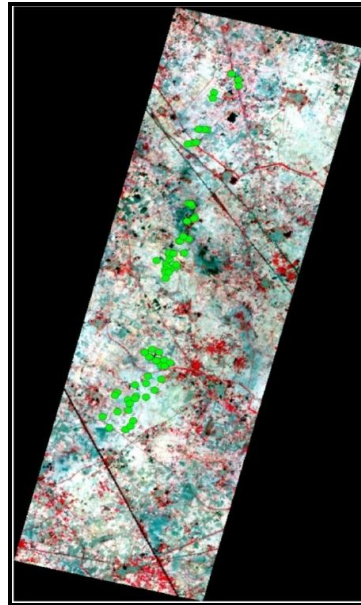


Figure 5: FCC Image of Study Area with Soil Sampling Points

#### 4.4. Soil Sample Collection, Analysis and Characterization

A detailed description about the soil sample collection, analysis and characterization are given by Suresh Kumar et al (2015). In total, 64 soil samples were collected from three transects of which 14 were normal, 14 were slight, 15 were moderate and 21 were high saline soils based on EC values. The general physico-chemical properties of the collected samples are given in Table 5.

Table 5: Physico-Chemical Characteristics of the Study Area

Soil Type (No. of Samples)	Texture	Organic Carbon (%)	pH (1:2)	EC(1:2) (dS/m)
Normal (14)	Loam-clay loam	0.16-1.32	6.87-8.22	0.16-3.07
Slight (14)	Loam-silt loam	0.16-0.93	7.68-8.40	4.28-7.70
Moderate (15)	Loam-clay loam	0.31-0.62	8.59 – 10.02	8.10 – 10.0
High (21)	Loam-silty clay loam	0.16-0.86	8.67- 10.20	10.21 – 30.41

#### 4.5. Spectral Indices Used in the Study

The various hyperspectral indices used in the study are listed in Table 6.

Table 6: The Spectral Indices Used in this Study

Spectral Indices	Equation	Reference
Soil Adjusted Vegetation Index (SAVI)	$SAVI = (1+L)(R_{864} - R_{660}) / (R_{864} + R_{660} + L)$	Huete (1988)
Normalized Difference Water Index (NDWI)	$(R_{864nm} - R_{1245nm}) / (R_{864nm} + R_{1245nm})$	Gao (1996)
Desertification Soil Index (DSI)	$(R_{1648nm} - R_{498nm}) / (R_{1648nm} - R_{2203nm} + 0.2)$	Wu et al (2010)
Salinity Index (SI)	$\sqrt{R_{436.99nm} * R_{630.32nm}}$	Suresh Kumar et al (2015)

#### 4.5.1. Soil Adjusted Vegetation Index (SAVI)

In areas where there are considerable soil brightness variations resulting from moisture differences, roughness variations, shadow, or organic matter differences, there are soil-induced influences on the vegetation index values (Huete, 1988). To account for such changes in soil optical properties, soil-adjusted vegetation indices have been developed. One of the widely used index is the Soil-Adjusted Vegetation Index (SAVI) given by Huete (1988), which incorporates a canopy background adjustment factor,  $L$ :

$$SAVI = (1+L) (R_{864} - R_{660}) / (R_{864} + R_{660} + L) \quad (1)$$

Where,  $R$  is the reflectance at the wavelengths denoted by the subscripts.  $L$  is a function of vegetation density and its determination requires knowledge of amount of vegetation present in the area. Determining the exact value of  $L$  for a particular situation involves iteration procedure. However, Huete (1988) suggested an optimal value of  $L=0.5$  to account for first-order soil background variations, as it was shown to reduce soil noise considerably throughout a wide range of vegetation densities.

#### 4.5.2. Normalized Difference Water Index (NDWI)

NDWI given by Gao (1996) was used in this study to differentiate the waterlogged areas from soil and vegetation areas. Exceptionally high values of NDWI indicate clear water surfaces and thus water logging can be effectively identified. Soil contribution to NDWI results in negative values whereas vegetation contribution results in positive values (Gao, 1996)

$$NDWI = (R_{864nm} - R_{1245nm}) / (R_{864nm} + R_{1245nm}) \quad (2)$$

#### 4.5.3. Desertification Soil Index (DSI)

It was given by Wu, et al. (2010) and was used in this study to assess the severity of soil degradation, based on the reflectance properties of the soil. The rationale behind the selection of reflectance at these particular wavelengths is described by Wu, et al. (2010).

$$DSI = (R_{1648nm} - R_{498nm}) / (R_{1648nm} - R_{2203nm} + 0.2) \quad (3)$$

**4.5.4 Salinity Index (SI):** Salinity index used in the study was proposed by Suresh Kumar, et al. (2015). This particular relationship was developed using the correlation studies between soil reflectance at various spectral bands and the salinity parameters ( $EC_e$ ). The calibration, validation and development of this salinity index was done using the same soil data set used in our study

$$SI = \sqrt{R_{436.99nm} * R_{630.32nm}} \quad (4)$$

#### 4.6. Support Vector Machine (SVM)

Support vector machines (SVMs) is a supervised non-parametric statistical learning technique, therefore makes no assumption about the probability distributions of the underlying data (analyzed data). In its original formulation (Vapnik, 1979), the method was presented with a set of labeled data instances and the SVM training algorithm aim to find a hyperplane that separate the dataset into a discrete predefined number of classes in a fashion consistent with the training examples. It separates the classes with a decision surface that maximizes the margin between the classes and thus minimizing misclassifications. The surface is often called the optimal separation hyperplane, and the data points closest to the hyperplane are called support vectors. These support vectors forms the key

elements of the training set. The essential idea underlying SVM is mapping the samples to the high dimensional kernel space non-linearly, and establishing the optimal hyperplane of low dimension in high dimensional kernel space (Mei, 2004).

In case of remote sensing data, SVM classification tries to identify the class associated with each pixel. It's useful in classification of complex and noisy data, as good results are obtained generally. They have the ability to successfully handle small training data sets and producing higher classification accuracies in comparison to traditional methods. Different types of kernels are applied in SVM method which can produce different types of training machines with non-linear hyperplanes and different results. Generally, four types of kernels are there: linear, polynomial, radial basis function (RBF) and sigmoid (ENVI, 2012). Of these RBF kernel was used in this study (Equation 5), as it yields higher accuracies in most of the cases,

$$K(x_i, x_j) = \exp(-\gamma \|x_i - x_j\|^2), \gamma > 0 \text{ (RBF)} \quad (5)$$

Where  $K(x_i, x_j)$  is called kernel function;  $x_i$  and  $x_j$  are training vectors

## 5. Results and Discussion

### 5.1. Soil Salinity Severity Mapping

All the four spectral index images were combined to form a new multiple band image using ENVI software. To develop salinity evaluation criteria, values of spectral indices were extracted from the well distributed GCP points, using the point map showing the various sampling sites. The range of spectral index values of various soil salinity classes were established as a salinity evaluation criteria (Table 7). SAVI sensitive to green vegetation was used to identify the healthy vegetation present in the study area, indicated with high values and confirmed by analyzing the spectral signature with ground truth. NDWI is sensitive to soil and vegetation water content and was used to differentiate soil and waterlogged areas. Very low NDWI values indicated soil aridity. Salinity index having high correlation with electrical conductivity (EC) can easily differentiate various salinity severity classes. Wide variation in the salinity index values helped to delineate various salinity classes more precisely. DSI values sensitive to degradation status of soil can reflect changes in soil salinity.

**Table 7:** Range of Spectral Index Values Associated With Various Salinity Classes

Salinity Classes	Spectral Indices			
	SAVI	NDWI	Salinity Index	DSI
Normal	>0.24	> -0.023	< 1250	< 4.0
Slight	0.18-0.24	-0.023 to - 0.055	1250-1450	4.0 – 6.65
Moderate	0.15-0.18	-0.055 to -0.073	1450-1600	6.65 – 7.8
High	< 0.15	< - 0.073	> 1600	> 7.8

#### 5.1.1. Soil Adjusted Vegetation Index (SAVI)

The SAVI image generated for the entire area showed a maximum value of 0.9 and a minimum of -0.08 (Figure 6). The area with higher values showed good vegetation cover even in the month of May, thus indicating regions having very low salinity. The values corresponding to vegetation areas were verified. A threshold value of 0.3 was taken to build mask for vegetation areas. The SAVI values varied under various salinity classes (Table 7), indicating the influence of salinity on vegetation.

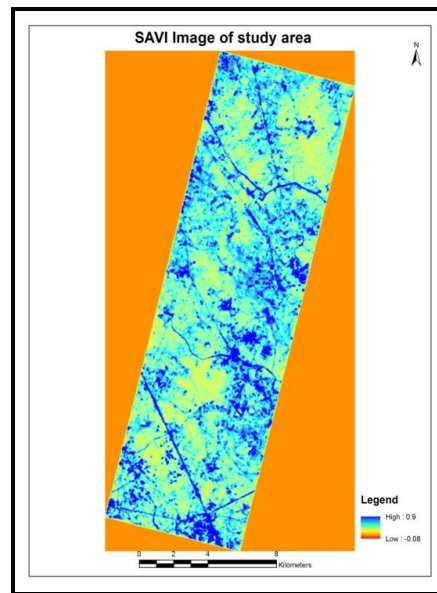


**Figure 6:** SAVI Image of Study Area

### 5.1.2. Normalized Difference Water Index (NDWI)

NDWI map of the study area showed a maximum value of 0.35 and minimum of -0.18 (Figure 7). Majority of the area had negative NDWI values, indicating contribution of soil and very low moisture in soil. Vegetation present in the area showed positive values of low magnitude. A threshold value of 0.1 was taken to build mask for waterlogged area in the study area. The NDWI of all the soil sampling sites were having negative value (Table 7). The NDWI values of highly saline soils were having the highest negative values compared to other classes, whereas normal soils have the lowest negative values, indicating some vegetation contribution to NDWI values thus driving them towards positive values.

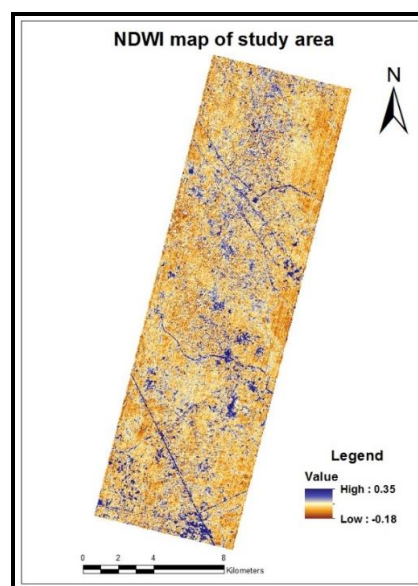


**Figure 7:** NDWI Map of Study Area

### 5.1.3. Desertification Soil Index (DSI)

DSI map of the study area showed positive values except in waterlogged areas (Figure 8). Higher values of DSI indicated high degradation of soil and poor vegetation cover. The range of DSI values under various salinity classes are shown in Table 7. With increasing salinity, the DSI values tend to increase may be due to the high contribution of salt content to the reflection in the corresponding wavelengths. Wu, et al. (2010) reported that the desertic soil has the highest DSI value, the bare land; wild grass ground and cultivated land have relatively high values (middle) while the vegetation and water bodies had low values. In this case, most of the area had DSI values in the middle range, except few points having very high value and waterlogged areas having low DSI values.

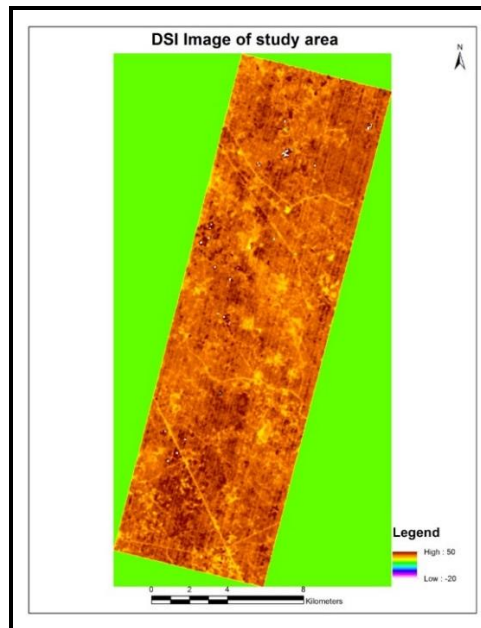


*Figure 8: DSI Image of Study Area*

### 5.1.4. Salinity Index (SI)

Salinity Index of the study area showed clear distinction between saline and non-saline or vegetation areas (Figure 9). High saline areas are having the highest SI values and normal soils having the least values. Suresh Kumar, et al. (2015) reported high correlation between salinity index and electrical conductivity values in the study area. It clearly stated that magnitude of the SI values can clearly distinguish between different salinity classes. The vegetation as well as waterlogged areas are having the least values for salinity index, thus it clearly showed the effect of salt content on reflectance properties.

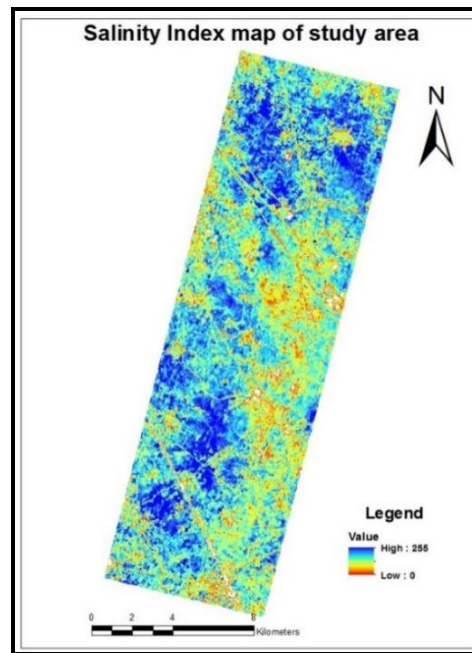


**Figure 9:** SI Map of Study Area

## 5.2. SVM Technique in Mapping Severity of Soil Salinity

Soil salinity severity map of the area was prepared using the SVM technique (Figure 10). Four spectral indices generated were stacked as layers and used for classification using SVM. The area was classified into four salinity severity classes i.e., normal, slight, moderate and high salinity classes. The region of interests (ROIs) was selected based on the data generated by soil sampling and further analysis of collected soil samples. The SVM parameters used in the study were kernel type, pyramid parameter and penalty parameter. The kernel type used was Radial Basis Function (RBF), Gamma in Kernel function was set to a value equal to the inverse of the number of the spectral bands used in classification with parameter defined as 0.25 (4 bands used), penalty parameter- 100, and classification probability threshold at 0. The pyramid parameter was set to a value of zero, forcing the various indices to be processed at full resolution. These parameters were defined by calibration with ground data as well as collected from literature (Wu, et al., 2010). The penalty parameter included in SVM allowed a certain degree of misclassification, which was particularly important for non-separable training sets. The penalty parameter controls the trade-off between allowing training errors and forcing rigid margins. It created a soft margin that permitted some misclassifications, such as it allowed some training points on the wrong side of the hyperplane. Increasing the value of the penalty parameter increases the cost of misclassifying points and forces the creation of a more accurate model that may not generalize well (ENVI, 2012) Classification probability threshold value set the probability that is required for the classifier to classify a pixel. Pixels where all rule probabilities are less than this threshold are unclassified. Here the value is set as 0, thus classifying all the pixels into one or the other class.

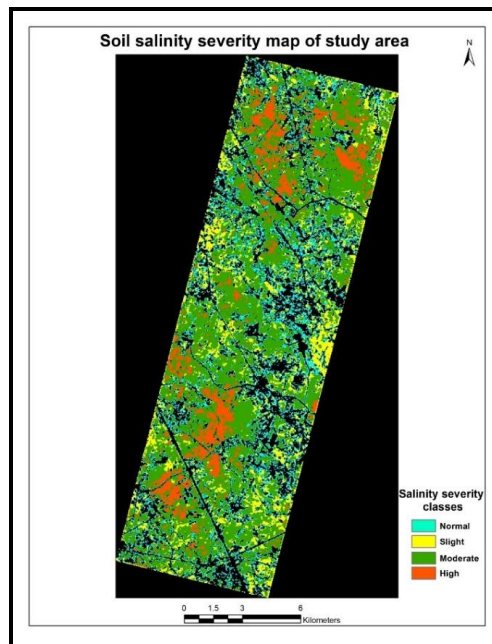


**Figure 10:** Soil Salinity Severity Map of Study Area

### 5.3. Accuracy Assessment

Classification accuracies of various salinity classes using SVM classification are shown in Table 8. A total number of 64 ground control points (GCPs) were used for accuracy assessment. 21 nos of GCPs belongs to highly salt affected, 15 nos of GCPs to moderately salt affected and 14 nos. of GCPs to slightly salt affected and normal soils were taken. The overall classification accuracy obtained was 78.13%, with a kappa statistic of 0.71. Salinity class wise accuracies were compared and we found high accuracies for soils of high salinity in comparison to other classes, attaining producers and users accuracies of 85.71% and 90.0% respectively. Slight saline class was having the lowest values for both producers and users accuracy, with values of 71.43% and 62.5% respectively, thus lowering the overall classification accuracy. The reflectance values of soils under slightly salt affected and normal areas were found to be very close and thus might have resulted in the mixing of these soils during classification, thus yielding lower accuracies. Whereas, the reflectance spectra of moderately and highly salt affected soils were evidently separated from other two classes, and thus had higher classification accuracies. The overall result showed that SVM classification approach employed has got very promising potential to discriminate various soil salinity severity classes, with high classification accuracies, when combined with high spectral resolution hyperspectral remote sensing data. The overall high accuracy produced by the SVM classifier may be attributed to the ability of the algorithm to identify the optimally separating hyperplanes for classes in comparison to other pixel-based techniques (e.g., artificial neural networks) (Licciardi, et al., 2009) which may not be able to find such optimal hyperplanes. SVMs are also able to generalize this optimal separating hyperplane to unseen samples with the least errors among all separating hyperplanes. This allowed them to produce the best class separation at the end of the classification (Huang, et al., 2002) The latter characteristic combined with the high spectral information provided by Hyperion at the pixel level resulted in a high overall classification accuracy using SVM.

**Table 8:** Accuracy Assessment of Soil Salinity Severity Classification Using SVM

Class Name	Reference	Classified	No. of Correct Classified	Producers Accuracy	Users Accuracy
Highly Salt affected	21	20	18	85.71	90.0
Moderately Salt affected	15	14	11	73.33	78.57
Slightly Salt	14	16	10	71.43	62.5
Normal Soil	14	14	11	78.57	78.57
<b>Overall Classification Accuracy = 78.13%</b>					
<b>Overall Kappa Statistics = 0.71</b>					

## 6. Conclusions

Hyperspectral remote sensing data is widely used in studies related to soil surface characterization and soil properties mapping especially, soil salinity severity. This forms a major remote sensing data source because of the high amount of information it can derive due to its high spatial as well as spectral resolution. It enables detailed study of various soil properties, which are not possible using multispectral remote sensing data. Various techniques like linear spectral unmixing, partial least square regression model, stepwise regression model, spectral angle mapper etc have been successfully used for studying soil salinity, using hyperspectral remote sensing data. Hyperspectral indices like SAVI, DSI, SI and NDWI were used for characterizing different classes of soil salinity. The results showed that these spectral indices are effective in distinguishing between various categories of salt affected soils. Among the four spectral indices used, Salinity index (SI) and Desertification Soil Index (DSI) were found to be more sensitive and thus respond very well to varying degrees of soil salinity and can be effectively used for clear distinction of various salinity classes. These indices when used for mapping of soil salinity severity using SVM method yielded maps of considerable accuracy. Soil salinity map showing different degrees of salinity prepared using SVM method achieved an overall accuracy of 78.13%, with the highest accuracies in case of highly salt affected soils and the least accuracies in slightly salt affected soil. It clearly points to the fact that soil salinity will make considerable changes in reflectance properties, only when present at certain higher amounts. At lower amounts of salinity, there are chances that the reflectance of normal as well as slightly salt affected soils will get mixed up and become indistinguishable resulting in errors during mapping. The validation of the accuracy assessment revealed reliable salinity severity class maps and correlate significantly with actual field conditions throughout the study area. The soil salinity severity map will help the planning and implementation of various soil management strategies for the effective reclamation of these soils and thereby improving crop production and effective utilization of land resources.

## References

- Abrol, A.P. and Bhumbra, D.R. *Saline and Alkali Soils in India- Their Occurrence and Management*. World Soil Resour, Rep. 1971. 41-42.
- Allbed, A. and Kumar, L. *Soil Salinity Mapping and Monitoring in Arid and Semi-Arid Regions Using Remote Sensing Technology: A Review*. *Advances in Remote Sensing*. 2013. 2; 373-385.
- Ben-Dor, E., Patkin, K., Banin, A. and Karnieli, A. *Mapping of Several Soil Properties Using DAIS-7915 Hyperspectral Scanner Data: A Case Study over Soils in Israel*. *International Journal of Remote Sensing*. 2002. 23 (6) 1043-1062.
- Csillag, F., Pasztor, L. and Biehl, L.L. *Spectral Band Selection for the Characterization of Salinity Status of Soils*. *Remote Sensing of Environment*. 1993. 43; 231-242.

Datt, B., Mc Vicar, T.R., Niel, T.G., Jupp, D.L. and Pearlman, J.S. *Preprocessing EO-1 Hyperian Hyperspectral Data to Support the Application of Agricultural Indexes*. IEEE Trans Geoscience Remote Sensing. 2003. 41; 1246-1259.

Dehaan, R.L. and Taylor, G.R. *Field-Derived Spectra of Salinized Soils and Vegetation as Indicators of Irrigation-Induced Soil Salinization*. Remote Sensing of Environ. 2002. 80; 406-417.

Dutkiewicz, A., Lewis, M. and Ostendorf, B. *Evaluation and Comparison of Hyperspectral Imagery for Mapping Surface Symptoms of Dry Land Salinity*. International Journal of Remote Sensing. 2009. 30; 693-719.

ENVI, 2012: ENVI User's Guide. Available online at: <http://www.RSInc.com/>

FAO, 2002: *Crops and Drops, Making the Best use of Water for Agriculture*. Food and Agriculture Organization of the United Nations, Rome, Italy.

Farifteh, J. and Van der Meer, F., 2005: *Spectral Characteristics of Salt-Affected Soils; Impact on Imaging, Spectroscopy*. 4th Workshop on Imaging Spectroscopy, April 27-29, Warsaw.

Gao, B.C. *NDWI: A Normalized Difference Water Index for Remote Sensing of Vegetation Liquid Water from Space*. Remote Sensing of Environment. 1996. 58; 257-266.

Ghosh, G., Kumar, S. and Saha, S.K. *Hyperspectral Satellite Data in Mapping Salt-Affected Soils Using Linear Spectral Unmixing Analysis*. Journal of Indian Society of Remote Sensing. 2012. 40; 129-136.

Hamzeh, S., Naseri, A.A., AlaviPanah, S.K., Mojaradi, B., Bartholomeus, H.M., Clevers, J.G.P.W. and Behzad, M. *Estimating Salinity Stress in Sugarcane Fields With Space Borne Hyperspectral Vegetation Indices*. International Journal of Applied Earth Observation and Geoinformation. 2012.

Huang, C., Davis, L.S. and Townshend, J.R.G. *An Assessment of Support Vector Machines for Land Cover Classification*. International Journal of Remote Sensing. 2002. 23; 725-749.

Huete, A.R. *A Soil-Adjusted Vegetation Index (SAVI)*. Remote Sensing of Environment. 1998. 25; 295-309.

Jian, Wu., Yaolin, Liu., Jing, Wang, and Ting, He. *Application of Hyperion Data to Land Degradation Mapping in the Hengshan Region of China*. International Journal of Remote Sensing. 2010. 31:19; 5145-5161.

Kumar, S., Gautam, G. and Saha, S.K. *Hyperspectral Remote Sensing Data Derived Spectral Indices in Characterizing Salt Affected Soils: A Case Study of Indo-Gangetic Plains of India*. Environmental Earth Sciences. 2015. 73; 3299-3308.

Licciardi, G.F., Pacifici, D., Tuia, S., Prasad, T., West, F., Giacco, Ch., Thiel, J., Inglada, E., Christophe, J., Chanussot and P .Gamba. *Decision Fusion for the Classification of Hyperspectral Data: Outcome of the 2008 GRS-S Data Fusion Contest*. IEEE Transactions on Geoscience and Remote Sensing. 2009. 47 (11) 3857-3865.

Mantero, P., Moser, G. and Serpico, S.B. *Partially Supervised Classification of Remote Sensing Images through SVM-Based Probability Density Estimation*. IEEE Transactions on Geoscience and Remote Sensing. 2005. 43 (3) 559-570.

- Mei, J.X., 2004: *Study on Object Detection for High Resolution Remote Sensing Images Based on Support Vector Machines*. PhD Thesis. Wuhan University, China.
- Metternicht, G. and Zinck, J.A. *Remote Sensing of Soil Salinity: Potentials and Constraints*. Remote Sensing of Environment. 2003. 5812; 1-10.
- Mitran, T., Ravisankar, T., Fyzee, M.A., Suresh, J.R., Sujatha, G. and Sreenivas, K. *Retrieval of Soil Physicochemical Properties Towards Assessing Salt-Affected Soils Using Hyperspectral Data*. Geocarto International. 2015.
- Mougenot, B. and Pouget, M. *Remote Sensing of Salt Affected Soils*. Remote Sensing Reviews. 1993. 7; 241-259.
- Oosterbaan, R.J., Sharma, D.P., Singh, K.N. and Rao, K.V.G.K. *Crop Production and Soil Salinity: Evaluation of Field Data from India by Segmented Linear Regression with Breakpoint*. Proceedings of the Symposium on Land Drainage for Salinity Control in Arid and Semi-arid regions. 1990. 3; Session V 373-383.
- Shahbaz, M. and Ashraf, M. *Improving Salinity Tolerance in Cereals*. Critical Reviews in Plant Science. 2013. 32; 237-249.
- Shepherd, K.D. and Walsh, M.G. *Development of Reflectance Spectral Libraries for Characterization of Soil Properties*. Soil Science Society of America Journal. 2002. 66; 988-998.
- Shi, Z. and Huang, M.X. *Evaluating Reclamation Levels of Coastal Saline Soil Using Laboratory Hyperspectral Data*. Eurasian Soil Science. 2007. 40; 1095-1101.
- Shrestha, D., Margateb, D.E., van der Meer, F. and Anhc, H.V. *Analysis and Classification of Hyperspectral Data for Mapping Land Degradation: An Application in Southern Spain*. International Journal of Applied Earth Observation and Geoinformation. 2005. 7 (2) 85-96.
- Szabolcs, I. *Salt-affected Soils*. CRC Press, Boca Raton, FL. 1989.
- Taylor, G.R. and Dehaan, R. *Image-Derived Spectral End Members as Indicators of Salinization*. International Journal of Remote Sensing. 2003. 24; 775-794.
- Toth, T., Csillag, F., Biehl, L. L. and Micheli, E. *Characterization of Semi Vegetated Salt-Affected Soils by Means of Field Remote Sensing*. Remote Sensing of Environment. 1991. 37; 167-180.
- Vapnik, V., 1979: *Estimation of Dependences Based on Empirical Data*. Nauka, Moscow. 5165-5184, 27 (in Russian) (English Translation: Springer Verlag, New York, 1982).